JCTC Journal of Chemical Theory and Computation

Computational Study of Tungsten(II)-Catalyzed Rearrangements of Norbornadiene

Allan L. L. East,* Greg M. Berner, Adam D. Morcom, and Lynn Mihichuk*

Department of Chemistry and Biochemistry, University of Regina, Regina, Saskatchewan S4S 0A2, Canada

Received March 12, 2008

Abstract: Rearrangements of norbornadiene (NBD, C_7H_8) to various alkylidenes, via a hypothetical 7-coordinate tungsten(II) complex $W(CO)_3I_2$(NBD), were studied using density-functional theory computations. An extensive search for intermediates and transition states of rearrangement was made. The theoretical method (basis sets and level of DFT) used was justified by new benchmark studies which compare optimized structural parameters to those from crystal structures of several different tungsten complexes. Transition-metal-catalyzed rearrangements of NBD are not as well-known as those of norbornene and are considerably more complicated than had been thought. This work predicts a large variety of intermediates which may be feasible targets for experimental synthesis. All the rearrangement paths to alkylidenes found here feature high activation energies of over 45 kcal mol^{-1}, implying that self-initiation for the ring-opening metathesis polymerization of NBD via tungsten(II) complexes must occur via an alternative mechanism.

Introduction

Norbornadiene (NBD, a C_7H_8 isomer) can undergo ring-opening metathesis polymerization (ROMP) via homogeneous catalysis by Group 6 transition-metal complexes without the need of a preformed metal carbene.[1–5] The propagation (metathesis) step is shown in Figure 1, with a tungsten catalyst WL_x, and proceeds via a metallacyclobutane structure as originally postulated by Hérisson and Chauvin.[6]

An outstanding mystery is the nature of the NBD rearrangement on the "unprepared" (i.e., nonmetal-carbene) catalyst to generate the required initial carbene (alkylidene). In the simpler case of the ROMP of norbornene (NBE) on similar catalysts, the activation step is believed[5,7] to be a net 1,2-H-shift along the metal-coordinated C═C double bond, based on experimental evidence.[8] However, NBD offers other possibilities due to its extra degree of unsaturation, and experimental evidence is even less clear-cut.[3] The only computational quantum-chemistry applications of the NBD rearrangement mechanism to date are the exploratory density-functional-theory (DFT) ones of Handzlik, Szymańska-Buzar, and co-workers.[9,10] Their most recent paper concludes that there are many possible rearrangements, that an acceptable mechanism remains elusive, and that more study is required.[10] Our study, begun before ref 10 was in print, fortuitously anticipated this call.

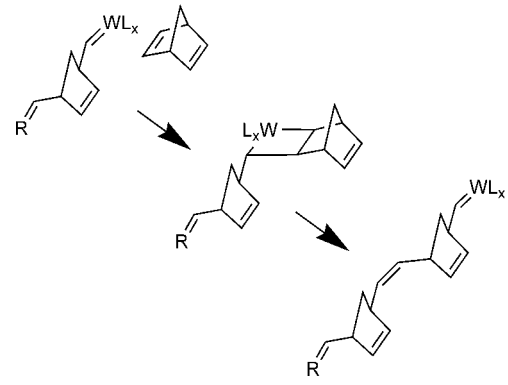

Figure 1. Propagation step in the ROMP of norbornadiene.

We set out to use DFT to thoroughly explore single-NBD rearrangements on an L_5W(NBD) complex, i.e. hypothesis category I of the four plausible ones presented in Figure 2. Our system of interest is $W(CO)I_2(\eta^2$-dppm$)(\eta^4$-NBD) (dppm

* Corresponding author e-mail: (A.L.L.E) allan.east@uregina.ca, (L.M.) lynn.mihichuk@uregina.ca.

10.1021/ct800088e CCC: $40.75
Published on Web 07/02/2008

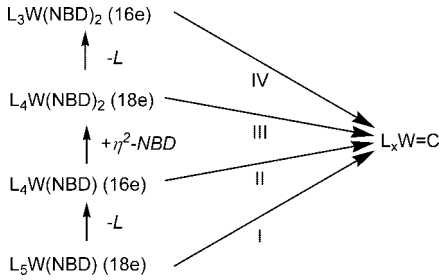

Figure 2. Four hypothesis categories for initial carbene generation, based on starting complex. Each category contains several hypothetical mechanisms to be explored; the present work studied category I.

$= Ph_2PCH_2PPh_2$), a known ROMP system,[11] but a complex far too large for thorough computational transition-state exploration for C_7H_8 rearrangement. Instead, we performed the transition-calculations with the analogous stereoisomer of the model complex $W(CO)_3I_2(\eta^4\text{-NBD})$. This "small-model approximation" is well justified for three reasons: (i) the qualitative mechanism for initial carbene generation should be fairly model-independent, since several Group 6 M-NBD complexes are capable of self-initiation,[1,2,10] (ii) our results contain a subset that qualitatively match the limited results of ref 10 for $Mo(CO)_3Cl(SnCl_3)(NBD)$ and $Mo(CH_3CN)(CO)_2Cl(SnCl_3)(NBD)$,[10] and (iii) our limited collection of computed intermediates for the dppm-containing system has been found using the smaller $W(CO)_3I_2(\eta^4\text{-NBD})$ system.

Our data are laid out as follows. First are data from several collected basis sets and levels of theory, which were benchmarked by using them to optimize the geometries of complexes for which there exists experimentally measured geometrical data: $W(CO)_6$,[12,13] *trans*-$W(CO)_4(\eta^2\text{-}C_2H_4)_2$,[14] $W(CO)_4(\eta^4\text{-NBD})$,[15] and the seven-coordinate tungsten(II) structure $W(CO)_3I_2(NCMe)_2$.[16] Second are data for NBD rearrangement in the model system $W(CO)_3I_2(\eta^4\text{-NBD})$: geometry-optimized energies and pathways for a large variety of transition states and intermediates that connect this reactant to various metal carbene intermediates, using the most successful theoretical method from the benchmarking study. Third is a brief data comparison to calculated data of other Group 6 M-NBD complexes, supporting our hypothesis that the DFT-approximated mechanism appears to be largely independent of the complex used.

Theoretical Methods

All calculations were performed using the Gaussian 03 software package.[17] Several levels of theory and basis sets were used in the preliminary benchmarking study. The theoretical method denoted BP86/RDZP:ITZ2DF:6−31G(d), as explained below, was chosen and used for the ensuing reaction-path study, and all energies are reported without zero-point corrections.

Levels of theory included the three density functional theory (DFT) approximations B3LYP,[18,19] BLYP,[19,20] and BP86[20,21] as well as the Møller−Plesset second-order perturbation theory (MP2),[22] and the expensive but very accurate coupled-cluster approximation CCSD(T).[23]

The basis set 6−31G(d)[17] was employed for all atoms except the large W and I atoms. Basis sets for W atoms all employed the Hay-Wadt small-core relativistic effective core potential,[24] which replaces all W core electrons up to 4*s*4*p*4*d*4*f*; hence, basis functions are needed for the 5*s* and 5*p* "core" as well as the 6*s*, 5*d*, and 6*p* valence orbitals. We tested the well-known Los Alamos LANL2MB[24] and LANL2DZ[17] basis sets as well as new even-tempered[25] sets developed by us at the University of Regina (RDZ, RDZP, RTZ, and RTZP, see the Appendix). The new sets were developed principally to add polarization functions but also to demonstrate that simple even-tempered basis sets work just as well as optimized ones for obtaining molecular geometries. For the I atom, three basis sets were used: (i) the LANL2DZ[17] basis set, with its complete-core relativistic effective core potential,[26] and two modifications proposed by Glukhovtsev et al.[27] which East and co-workers have used before, [28] (ii) LANL2DZ with added *d*- and *f*-orbital polarization functions (LANL2DZDF), and (iii) a triple-ζ uncontraction of the *s* and *p* sets with added 2*d* and 1*f* polarization sets (ITZ2DF).

Transition-state calculations were optimized for $W(CO)_3I_2NBD$ using the eigenvector−following transition-state algorithm (TS,EF).[29] However, since the TS,EF algorithm in G03 allows for simultaneous optimization of no more than 50 of the 66 geometry variables, several others were held fixed during the optimizations: carbonyl-group coordinates and/or H-atom coordinates of rigid H atoms in the NBD group. Each optimized transition state was subjected to a vibrational frequency analysis, to ensure that the magnitudes of the positive and one imaginary frequency were greater than the residual noise (the six "zero frequencies" for translations and rotations from normal mode diagonalization). Each one was also verified by two energy-minimization runs, begun from geometries displaced from the transition state (0.05 Å or 5−10°), which more definitively identifies the two intermediates that it connects. This precaution was essential, for we routinely discovered extra and unexpected intermediates in this manner.

Results and Discussion

Tungsten Basis Set Benchmarking. Four new and two traditional basis sets for tungsten orbitals were tested for their ability to reproduce experimental gas-phase[12] or crystal-phase[13] bond lengths of $W(CO)_6$ (Table 1).

Note from the experimental values that crystal-packing effects[30] reduce R_{WC} and R_{CO} by 0.033 and 0.003 Å, respectively, from their gas-phase values. Computed results for an isolated molecule should be properly compared with gas-phase results, and this comparison for values of R_{WC} reveals that the Regina double-ζ basis sets strike the best balance with B3LYP, but the LANL2DZ basis set performs better when paired with BP86 or the ab initio non-DFT method MP2. Note that a different choice, MP2/RDZP, performs best if one is instead interested in a level of theory that gives the best agreement with crystal-phase bond lengths.

The computed carbonyl R_{CO} values are hardly affected by the basis set choice for tungsten. These R_{CO} values are all

Table 1. Computed Bond Lengths (Å) and Percent Errors for $W(CO)_6$

level of theory	W basis set	W-CO (Å)	% error vs crystal	% error vs gas	C−O (Å)	% error vs crystal	% error vs gas
B3LYP	RDZ	2.060	1.7	0.1	1.151	0.5	0.3
	RDZP	2.058	1.6	0.0	1.151	0.5	0.3
	RTZ	2.069	2.2	0.5	1.152	0.6	0.3
	RTZP	2.068	2.1	0.5	1.152	0.6	0.3
	LANL2MB	2.071	2.3	0.6	1.150	0.4	0.2
	LANL2DZ	2.068	2.1	0.5	1.150	0.4	0.2
BLYP	RDZP	2.067	2.1	0.4	1.165	1.7	1.5
	RTZP	2.077	2.6	0.9	1.166	1.8	1.6
	LANL2DZ	2.076	2.5	0.9	1.165	1.7	1.5
BP86	RDZP	2.052	1.3	−0.3	1.164	1.7	1.4
	RTZP	2.062	1.8	0.2	1.165	1.7	1.5
	LANL2DZ	2.061	1.8	0.1	1.164	1.7	1.4
MP2	RDZP	2.033	0.4	−1.2	1.167	1.9	1.7
	RTZP	2.041	0.8	−0.8	1.168	2.0	1.7
	LANL2DZ	2.053	1.4	−0.2	1.166	1.8	1.6
CCSD(T)	RDZP	2.058	1.6	0.0	1.159	1.2	1.0
experiment[12]	(gas)	2.058			1.148		
experiment[13]	(crystal)	2.025(8)			1.145(15)		

systematically high, due both to the small basis set used for C and O (6−31G(d)) and the moderate level of theory. We also performed a high-level CCSD(T) optimization, which showed improvement in R_{CO} and the adequacy of the new RDZP basis set for tungsten.

Since we also desired a tungsten basis set appropriate for η^2 interactions of C═C double bonds with W, we further tested the RDZP, RTZP, and LANL2DZ sets on the R_{WC} distances to alkene carbons in *trans*-$W(CO)_4(\eta^2\text{-}C_2H_4)_2$ and $W(CO)_4(\eta^4$-NBD) (Figure 3).[14,15] The RDZP basis set outperformed the others with DFT methods, producing errors of less than 1.2% when used with either B3LYP or BP86.

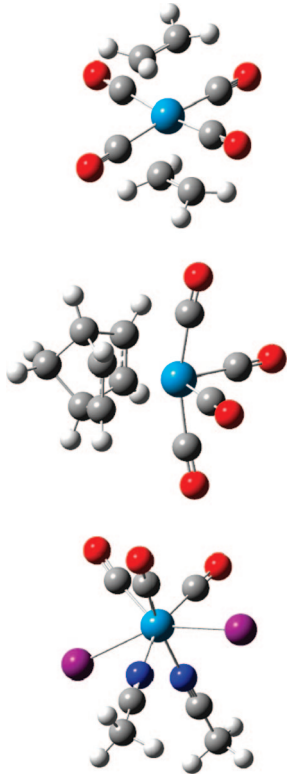

Figure 3. Structures of *trans*-$W(CO)_4(\eta^2\text{-}C_2H_4)_2$, $W(CO)_4(\eta^4$-NBD), and $W(CO)_3I_2(NCMe)_2$, optimized via BP86/RDZP:ITZ2DF:6−31G(d).

Iodine Basis Set Benchmarking. In order to test potential iodine basis sets in conjunction with the already established W basis sets and to extend our tests to a 7-coordinate complex, optimizations of the complex $W(CO)_3I_2(NCMe)_2$ (see Figure 3) were performed. The optimizations were conducted using the B3LYP, BP86, and MP2 levels of theory with the RDZP, RTZP, and LANL2DZ mixed basis sets for W each combined with the ITZ2DF, LANL2DZ, and LANL2DZDF basis sets for I. Computed bond lengths to W and percent error data for these computations are presented in Table 2. The experimental data[16] for $W(CO)_3I_2(NCMe)_2$ show two degenerate R_{WC} values ("long") and two degenerate R_{WN} values; hence, for comparisons, we averaged the near-degenerate computed values in these cases.

In comparing the results from optimizations using the LANL2DZ and LANL2DZDF basis sets for I it was found that the added *d* and *f* polarization functions significantly improved the accuracy. As a result it was decided to try yet another basis set for W, by adding *f*-polarization to LANL2DZ (LANL2DZF). These results are also shown in Table 2, and although the polarization functions did provide an improvement over the optimizations performed with LANL2DZ, it did not lead to the optimal method. The optimal method, which kept all R_{WX} percent errors (relative to experimental crystal-structure values) at or below 2.4%, was BP86/RDZP:ITZ2DF:6−31G(d), and this was the level of theory chosen for the rearrangement study.

$W(CO)_3I_2(\eta^4$-NBD) and Intermediates. We found over 40 different minimum-energy structures and speculate that over 100 probably exist. Broadly, these structures could be grouped in three classes: (i) ordinary π-complexes of stable alkenes, (ii) alkylidenes (carbenes), and (iii) C−H and C−C insertion (oxidative addition) compounds. Figure 4 provides summary sketches of the structures obtained, while full images (top and side views) are provided in the Supporting Information. Computed relative energies (no zero-point corrections) appear in Table 3.

The alkenes we considered were the NBD reactant, in η^4 (**1**) and η^2 (**2**) forms, and two vinylcyclopentadienes (**3**, **4**) which are closely related to the diene alkylidenes (**9**, **10**).

Table 2. Computed Bond Lengths (Å) and Percent Errors for $W(CO)_3I_2(NCMe)_2$ Using Various Methods and Heavy-Atom Basis Sets

W basis set	I basis set	W−I short	W−I long	W−CO short	W−CO long	W−N	max % error
			B3LYP				
RDZP	ITZ2DF	2.865	2.941	1.990	1.993	2.176	3.3
	LANL2DZDF	2.865	2.941	1.988	1.992	2.177	3.3
	LANL2DZ	2.916	2.962	1.982	2.002	2.173	4.3
RTZP	ITZ2DF	2.865	2.947	2.001	2.005	2.190	3.6
	LANL2DZDF[a]	2.864	2.946	2.001	2.005	2.191	3.5
	LANL2DZ[a]	2.888	2.978	2.000	2.005	2.188	4.6
LANL2DZ	ITZ2DF	2.882	2.963	2.003	2.007	2.197	4.1
	LANL2DZDF	2.887	2.969	2.003	2.006	2.197	4.4
	LANL2DZ	2.926	3.015	2.003	2.007	2.193	5.9
LANL2DZF	LANL2DZDF[a]	2.875	2.949	1.993	1.999	2.200	3.6
			BP86				
RDZP	ITZ2DF	2.845	2.915	1.986	1.989	2.152	2.4
	LANL2DZDF[a]	2.845	2.917	1.985	1.987	2.152	2.5
	LANL2DZ	2.877	2.956	1.983	1.986	2.150	3.9
RTZP	ITZ2DF	2.844	2.923	1.998	2.000	2.166	2.7
	LANL2DZDF	2.845	2.923	1.997	1.999	2.167	2.7
	LANL2DZ[a]	2.870	2.955	1.996	1.999	2.165	3.8
LANL2DZ	ITZ2DF[a]	2.860	2.941	1.999	2.000	2.173	3.3
	LANL2DZDF	2.866	2.946	1.999	2.000	2.173	3.5
	LANL2DZ	2.906	2.992	1.997	2.000	2.170	5.1
LANL2DZF	ITZ2DF	2.850	2.923	1.989	1.992	2.176	2.7
	LANL2DZDF	2.856	2.922	1.991	1.994	2.175	2.7
			MP2				
RDZP	ITZ2DF	2.777	2.821	1.960	1.965	2.146	3.3
	LANL2DZDF	2.769	2.813	1.957	1.963	2.148	3.4
	LANL2DZ	2.812	2.845	1.949	1.958	2.146	3.7
RTZP	ITZ2DF	2.773	2.824	1.969	1.974	2.154	2.9
	LANL2DZ	2.790	2.830	1.961	1.968	2.152	3.2
LANL2DZ	ITZ2DF	2.821	2.863	1.971	1.979	2.175	2.7
	LANL2DZDF	2.824	2.861	1.967	1.976	2.171	2.8
	LANL2DZ	2.880	2.910	1.962	1.971	2.163	3.1
experiment[16]	(crystal)	2.797	2.846	1.99	2.03	2.17	

[a] These computations were assessed converged; automatic convergence failed due to continually large displacements of nearly free methyl rotation modes.

The regular (**2a**) and inverted (**2b,c**) η^2-NBD complexes are 17 and 12−13 kcal mol^{-1} higher in energy than the η^4-NBD reference point **1**, at the BP86 level of DFT used here.

The alkylidene structures could be further subdivided into tricyclic no-ene (**5**), bicyclic monoene (**6**−**8**), and monocyclic diene (**9**, **10**) versions. The lowest-energy versions were **5** and **6**, being only 1 and 5−6 kcal mol^{-1} above **1**. The monocyclic diene alkylidenes **9** and **10** exhibited both ring-η^2 backbiting (**9a**, **9d, 9e, 10a**, **10b, 10e**) and nonbackbiting (**9b**, **9c**, **10c**, **10d, 10f**) forms, with the ring-η^2 interaction providing 3−6 kcal/mol of extra stabilization. One of our attempts at an alkylidene resulted in carbene insertion into a nearby carbonyl group, resulting in an η^2-ketene (**11**).

The C−H bond insertions resulted in various positions for the H atom, depending on the nearby ligands: a simple W−H bond (**12**), μ-bridging I and I (**13**), or μ-bridging W and C (**14**). In one case, the insertion resulted in new C−C bond formation between C_7H_7 and a carbonyl group in an acyl fashion (**15**).

The C−C bond insertions result in an exotic mix of structures having two connections from C_7H_8 to W, and the lowest-energy ones were quadricyclane-like dialkyl intermediates (**16a,b**) lying 11−13 kcal mol^{-1} above **1**, and three π-allyl (η^3-allyl) intermediates (**20a, 21b, 22a**) lying 9−12 kcal mol^{-1} above **1**.

Experimentally, none of these types of W-containing intermediates have been isolated. Tungsten(II)-alkylidene structures **5**−**10** and the C−C-insertion intermediates **16**−**23** would be highly reactive in the presence of excess hydrocarbons, and the C−H-insertion intermediates **12**−**15** would be highly reactive because they are high in energy. Ruthenium versions of the vinylcyclopentadiene π-complexes **3** and **4** have been observed as results of Ru-NBD rearrangements.[31] The π-allyl structures **20**−**23** might be experimentally isolable, since their energies are moderate, and organometallic complexes with π-allyl C_3H_5 ligands have been prepared.[32]

Rearrangements via C−H Bond Insertions. Results for C−H insertion routes appear in Figure 5. Routes to alkylidenes tended to involve H-atom transfer to the catalyst, followed by its back-transfer to a different carbon atom on the C_7H_7 moiety to produce bicyclic or tricyclic carbenes. However, Figure 5 shows that we never actually found a 2-step mechanism from the η^4-NBD structure **1**. Two-step mechanisms from η^2-NBD structures were found. The lowest-barrier paths to alkylidenes found were one-step ones: one from **1** to **6b** and one from **2b** to **6b**. All of the paths to alkylidenes here require rather high activation barriers of over 45 kcal mol^{-1}.

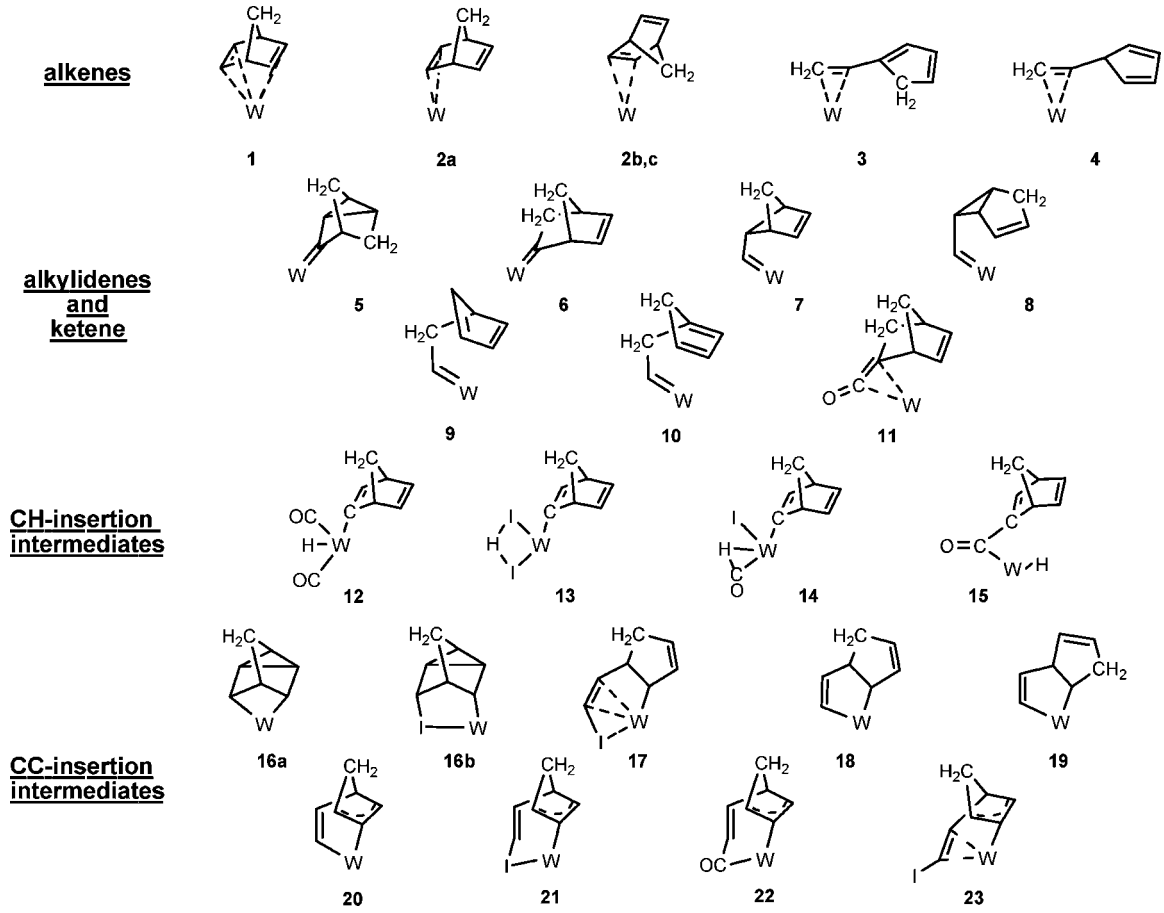

Figure 4. Structures found as intermediates (local minima) in this work.

Table 3. Computed Relative Energies (kcal mol^{-1}) for Intermediates of $WI_2(CO)_3(C_7H_8)$

structure	E	structure	E	structure	E	structure	E
1	0.0	**8b**	19.0	**10f**	11.7	**19**	43.4
2a	17.1	**9a**	15.7	**11**	22.6	**20a**	8.9
2b	12.2	**9b**	22.1	**12a**	34.8	**20b**	23.8
2c	13.4	**9c**	27.3	**12b**	34.1	**21a**	15.0
3	−2.6	**9d**	7.7	**13**	42.4	**21b**	12.0
4	11.8	**9e**	7.1	**14**	44.3	**22a**	10.2
5	1.1	**10a**	38.7	**15**	40.6	**22b**	15.8
6a	5.9	**10b**	14.9	**16a**	13.1	**23**	26.0
6b	5.4	**10c**	18.1	**16b**	11.5		
7	34.3	**10d**	19.2	**17**	33.8		
8a	16.5	**10e**	5.5	**18**	32.3		

The route we accidentally found to the ketene **11** was a surprise, as it came in one step from NBD without first forming an alkylidene. The barrier for this direct step is quite high, however, at 71 kcal mol^{-1}.

Rearrangements via C−C Bond Insertions. Results for C−C insertion routes appear in Figure 6. Four of the six routes to alkylidenes involved intermediates with σ-vinyl + π-allyl interactions to the catalyst (**20**−**22**). The six C−C insertion routes resulted in either monocyclic carbenes **9** and **10** or the peculiar bicyclic carbene **8a** with a 3-membered ring; this is unlike the four C−H insertion routes which led to different bi- and tricyclic alkylidenes.

The routes via π-allyl structures **20a** and **20b** were clean 2-step processes in which the intermediate featured both vinyl and π-allyl interactions with the tungsten atom. The vinyl arm of C_7H_8 was positioned between two like ligands in these cases: two carbonyl groups in **20a** and two iodine atoms in **20b**. When we tried putting this vinyl arm between unlike groups, the mechanism became complex: it began with a non-π-allyl structure **17** and then branched to three different structures (**21a**, **18,** or **23**), two of which we successfully connected to alkylidenes.

We would like to point out the similarities between resonant η^3 π-allyl structures (**20**−**23**) and localized η^1 non-π-allyl ones (**17**−**19**). The localization of the resonance in **21** can lead to **17** without any H shifts, and localization of the resonance in **20** can similarly lead to either **18** or **19**. However, we see indications that such interconversions, while geometrically simple, may have sizable energy barriers: we cite the example of **17** to **21a** and the absence of **18** or **19** when the mechanism passes through **20a** or **20b**.

The η^3 π-allyl intermediates led directly to alkylidenes with a backbiting η^2 interaction with W, the structures on the left side of the gray area in Figure 6. The route to **10** via 1,2-H-shift has an insurmountable barrier of 90 kcal/mol, and hence structure **9** (via 1,3-H-shift) is favored over **10**. We also pursued the additional step of removal of the backbiting interactions in alkylidenes 8−10 (right side of gray area). We found that this could be done in two ways: the cyclopentadiene ring could either flip or shear away from the W atom. From structure **10b**, the flip barrier to **10d** was 3 kcal mol^{-1} lower than the shear barrier to **10c**. We only pursued shear steps for the other cases: **8a** to **8b** and **9a** to **9b**.

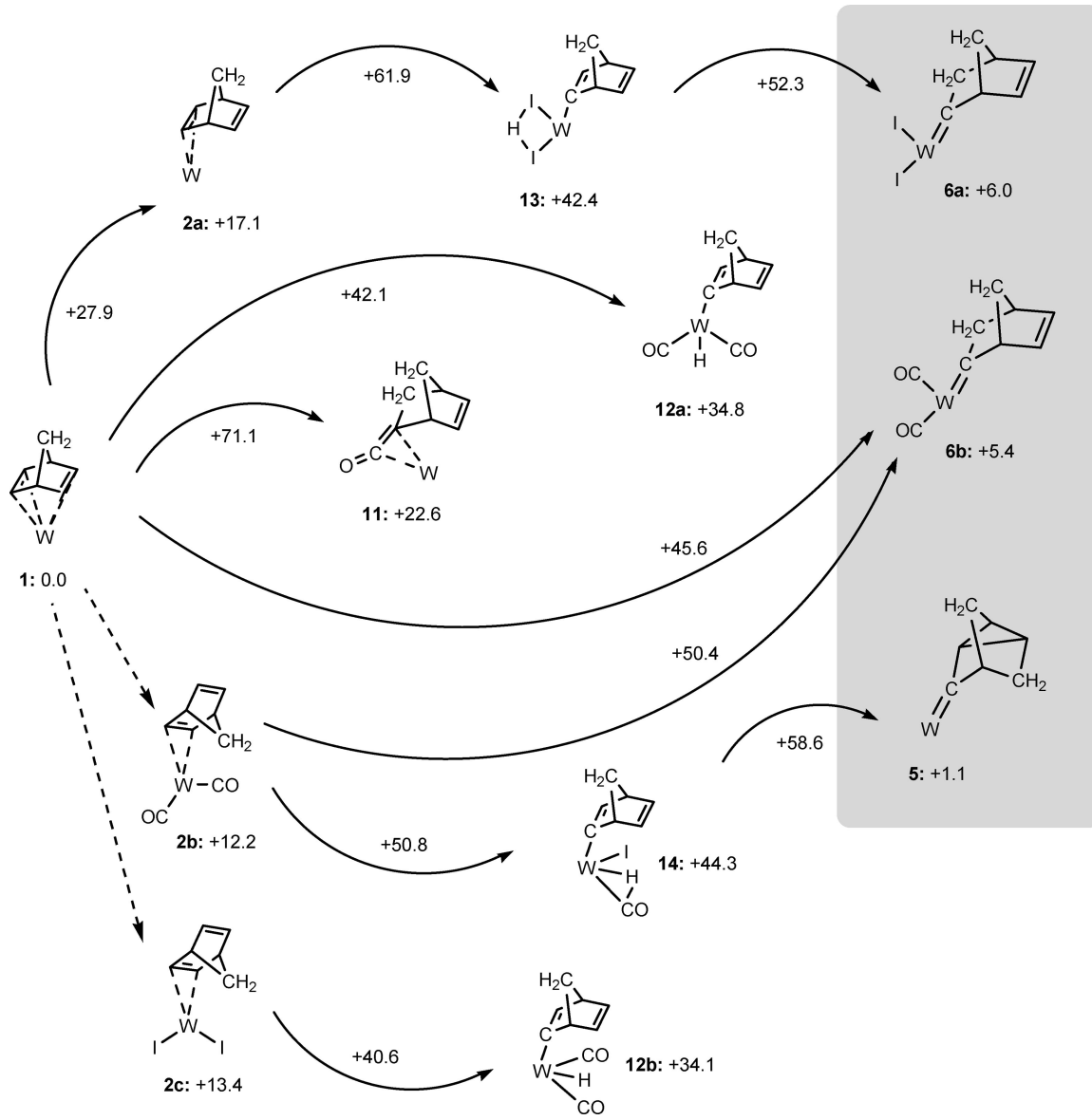

Figure 5. Reaction pathways via C−H insertion as found computationally. Alkylidene structures are in the gray area on the right. All energies are in kcal mol^{-1}; the ones alongside reaction arrows represent transition-state energies relative to **1** (i.e., not individual-step barrier heights).

Table 4. Overall Computed Energy Barriers (kcal mol^{-1}) for Selected Rearrangements of NBD to Alkylidenes via Group 6 Complexes

molecule	level of theory	**1** to **6**	**1** to **2?** to **6**	**1** to **16** to **8**	**1** to **17?** to **18** to **10**
$W(CO)_3I_2$(NBD), this work	BP86/mixed	45.6	50.4	53.5	61.9
$Mo(CO)_2$(MeCN)Cl($SnCl_3$)(NBD)[10]	B3LYP/LANL2DZ	49.2	52.3	47.6	59.5

All of our C−C insertion paths to alkylidenes also require rather high activation barriers, of over 50 kcal mol^{-1}.

Comparison to Results Using Other Group 6 M-NBD Complexes. Handzlik et al. recently published a limited computational study of NBD rearrangement, using B3LYP/LANL2DZ as the computational method and either $Mo(CO)_2$(MeCN)Cl($SnCl_3$)(NBD) or $Mo(CO)_3$Cl($SnCl_3$)-(NBD) as catalysts.[10] Of the single-NBD pathways they located, they present three (with 5 transition states) and discuss 3 others (with perhaps 4 transition states). Of these 6 paths, 4−6 appear to be among our 10 paths, hence strongly supporting our hypothesis that that mechanistic similarities should exist within a family of W(II) or Mo(II)-based catalysts.

The 4 paths of Handzlik et al. that are common to ours have similar large overall barrier heights, as shown in Table 4. Their single-NBD study was certainly not as thorough as ours, as we found three times as many transition states, and our intermediates **2**−**5**, **7**, **9**, **11**−**15**, **17**, and **19**−**23** are all new, with several being likely to exist with their Mo-based systems.

We have managed to obtain a BP86-optimized structure of the larger complex $W(CO)I_2(\eta^2$-dppm$)(\eta^4$-NBD) (dppm = $Ph_2PCH_2PPh_2$) as well as a few intermediate structures we

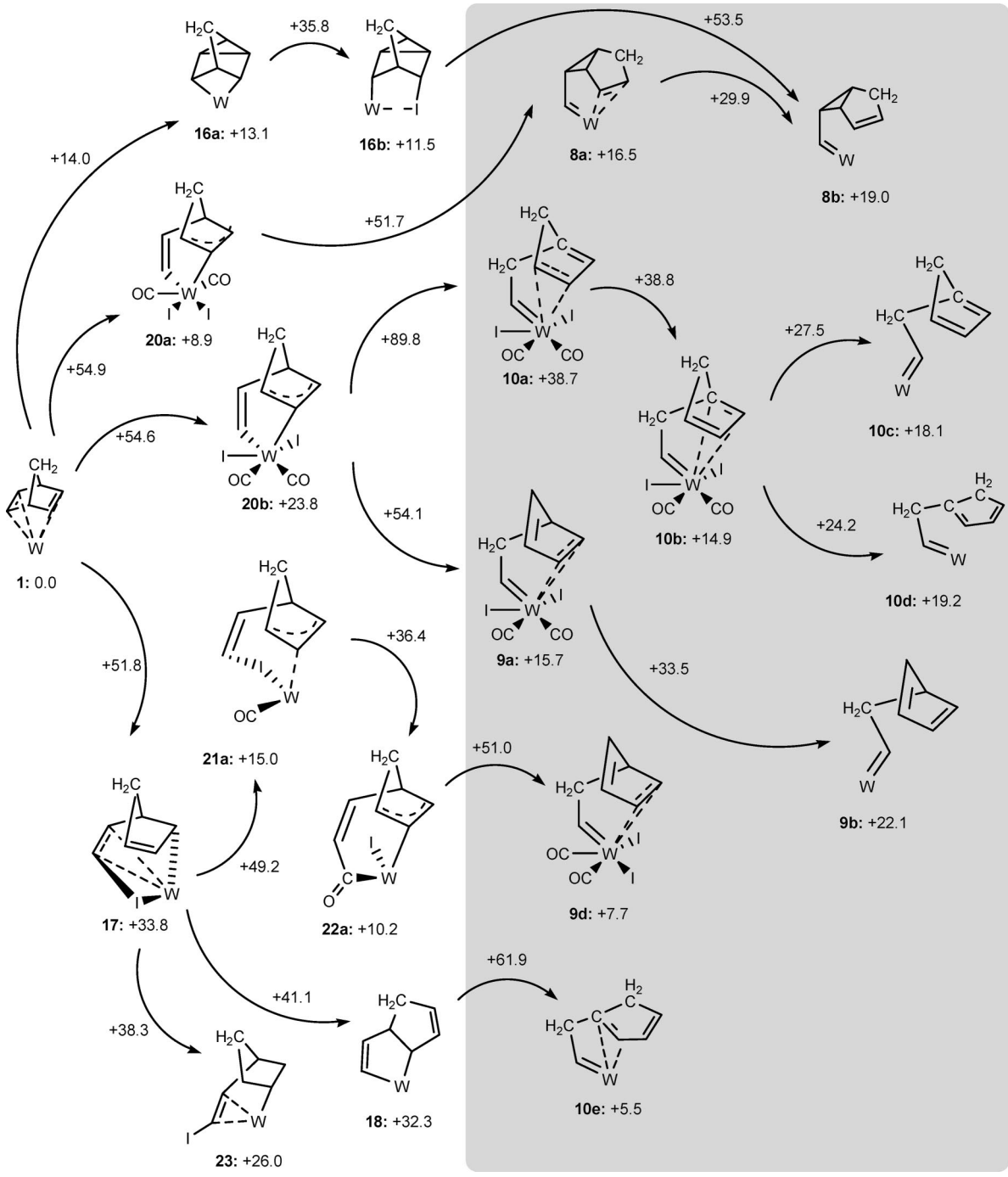

Figure 6. Reaction pathways via CC insertion as found computationally. Alkylidene structures are in the gray area on the right. All energies are in kcal mol^{-1}; the ones alongside reaction arrows represent transition-state energies relative to **1** (i.e., not individual-step barrier heights).

Table 5. Relative BP86 Energies (kcal mol^{-1}) of Intermediates of Two Tungsten(II) Systems

molecule	1	6a	34	8a	9b	10c	12a	16a
$W(CO)_3I_2(C_7H_8)$	0	6	34	17	22	18	35	13
$W(CO)I_2(\eta^2$-dppm$)(C_7H_8)$	0	14	40	29	19	11	46	24

obtained with the smaller $W(CO)_3I_2(\eta^4$-NBD) system. The same basis sets were used, except that STO-3G was used for the nonphosphorus atoms of dppm. No new intermediates were found with the larger system. Table 5 compares their relative energies. There is a general shift of 6−12 kcal mol^{-1}, likely due to steric effects of the bulky dppm ligand; the exceptions are in structures **9** and **10**, where the C_7H_8 moiety is more flexible and appears to benefit from π-π T-shaped stacking of its dangling cyclopentadiene ring with a phenyl group of dppm.

Conclusions

We make four main conclusions. (i) The BP86 DFT level of theory, with appropriate atomic basis sets, can reproduce crystalline organometallic R_{WX} bond lengths to within 2.4%. (ii) A large variety of intermediates should be considered as candidates in the rearrangement of a single norbornadiene with a tungsten(II) catalyst, and we hope that our Figure 4 will serve as a useful catalog for future studies. (iii) Generally, carbenes

Chart 1. W Atom, RDZP Set

```
W 0
S       3       1.00    0.000000000000
3.2400000000D+00        -0.5D+00
1.0800000000D+00        +0.9D+00
0.3600000000D+00        +0.5D+00
S       4       1.00    0.000000000000
3.2400000000D+00        +0.2D+00
1.0800000000D+00        -0.5D+00
0.3600000000D+00        -0.4D+00
0.1200000000D+00        +0.9D+00
S       1       1.00    0.000000000000
0.0400000000D+00        +1.0D+00
P       3       1.00    0.000000000000
3.2400000000D+00        -0.2D+00
1.0800000000D+00        +0.8D+00
0.3600000000D+00        +0.4D+00
P       2       1.00    0.000000000000
1.0800000000D+00        -0.3D+00
0.1200000000D+00        +0.3D+00
P       1       1.00    0.000000000000
0.0400000000D+00        +1.0D+00
D       2       1.00    0.000000000000
1.0800000000D+00        +0.3D+00
0.3600000000D+00        +0.5D+00
D       1       1.00    0.000000000000
0.1200000000D+00        +1.0D+00
F       1       1.00    0.000000000000
0.3600000000D+00        +1.0D+00
```

Chart 2. W Atom, RTZP Set

```
W 0
S       3       1.00    0.000000000000
3.2400000000D+00        -0.5D+00
1.0800000000D+00        +0.9D+00
0.3600000000D+00        +0.5D+00
S       3       1.00    0.000000000000
3.2400000000D+00        +0.2D+00
1.0800000000D+00        -0.5D+00
0.3600000000D+00        -0.4D+00
S       1       1.00    0.000000000000
0.1200000000D+00        +1.0D+00
S       1       1.00    0.000000000000
0.0400000000D+00        +1.0D+00
P       3       1.00    0.000000000000
3.2400000000D+00        -0.2D+00
1.0800000000D+00        +0.8D+00
0.3600000000D+00        +0.4D+00
P       1       1.00    0.000000000000
1.0800000000D+00        +1.0D+00
P       1       1.00    0.000000000000
0.1200000000D+00        +1.0D+00
P       1       1.00    0.000000000000
0.0400000000D+00        +1.0D+00
D       1       1.00    0.000000000000
1.0800000000D+00        +1.0D+00
D       1       1.00    0.000000000000
0.3600000000D+00        +1.0D+00
D       1       1.00    0.000000000000
0.1200000000D+00        +1.0D+00
F       1       1.00    0.000000000000
0.3600000000D+00        +1.0D+00
```

obtained via C−C bond insertion of NBD have (with one exception) a single cyclopentadiene ring, while carbenes obtained by C−H bond insertion of NBD remain bicyclic or become tricyclic. (iv) None of the rearrangement pathways found here had an activation barrier lower than 45 kcal mol^{-1}, suggesting that the ROMP of norbornadiene may *not* start with any of the rearrangements studied here.

On point (iv) we add the following remarks. Since our study dealt only with hypothesis category I (Figure 2), the other categories should be investigated. The exploratory calculation of a category III pathway by Handzlik et al.[10] produced an overall barrier of 35 kcal mol^{-1}, which is still high, but it is intriguingly lower than those of all the single-NBD rearrangements studied here. The ultimate goal of understanding the activation steps of ROMP will continue to benefit from additional careful computational research.

Acknowledgment. We thank the Natural Science and Engineering Research Council and the Canada Foundation for Innovation for funding and the Laboratory for Computational Discovery (Regina) for supercomputer maintenance. Dr. Szymańska-Buzar is thanked for alerting us to her latest manuscript while we were finishing our paper.

Appendix

The following Gaussian03-ready input files are for new sets of basis functions to represent the 5*s*, 6*s*, 5*p*, 6*p*, and 5*d* orbitals of W atom. The input files present columns of coefficients c_{ij} and exponents α_{ij} that define a contracted basis function Φ_i as a sum of primitive basis functions

$$\Phi_{ilm}(r,\theta,\varphi) = \sum_j c_{ij} e^{-\alpha_{ij} r^2} Y_l^m(\theta,\varphi)$$

where $Y_l^m(\theta,\phi)$ indicates a spherical harmonic function.

The first input file is for the RDZP set (see Chart 1): one contracted *s* function for the 5*s* orbital, a double-ζ pair of *s* functions for the 6*s* orbital, one contracted *p* function for each 5*p* orbital, a double-ζ pair for each 6*p* orbital, and a double-ζ pair for each 5*d* orbital. The final two lines represent the uncontracted set of polarization *f* functions, used in RDZP but removed for RDZ. The second input file is for the RTZP set (see Chart 2), with triple-ζ sets for the 6*s*, 6*p*, and 5*d* orbitals; again, the final uncontracted set of polarization *f* functions is used for RTZP but removed for RTZ.

These basis sets are based on a 5531 set of *spdf* primitive basis functions with very simple even-tempered exponents $\alpha_j = \alpha_{mid}\beta^{\pm j}$; our choice of $\alpha_{mid} = 0.36$ and $\beta = 3$ were made to span roughly the same exponent range as that of the LANL2DZ primitives. The coefficients c_{ij} in the contractions were chosen to mimic the Kohn−Sham atomic orbital coefficients observed in a B3LYP calculation for the ^{7}S state of W atom.

Supporting Information Available: Side and top views of each optimized intermediate of Table 3 and tables of Cartesian coordinates of all 30 transition states. This material is available free of charge via the Internet at http://pubs.acs.org.

References

(1) Amass, A. J.; McGourtey, T. A.; Tuck, C. N. *Eur. Polym. J.* **1976**, *12*, 93.

(2) Sen, A.; Thomas, R. R. *Organometallics* **1982**, *1*, 1251.

(3) (a) Szymańska-Buzar, T.; Głowiak, T.; Czeluśniak, I. *J. Organomet. Chem.* **2001**, *640*, 72. (b) Szymańska-Buzar, T.; Głowiak, T.; Czeluśniak, I. *Polyhedron* **2002**, *21*, 2505.

(4) Baker, P. K.; Drew, M. G. B.; Meehan, M. M.; Müller, J. *Z. Anorg. Allg. Chem.* **2002**, *628*, 1727.

(5) Bencze, L.; Bíró, N.; Szabó-Ravasz, B.; Mihichuk, L. *Can. J. Chem.* **2004**, *82*, 499.

(6) Hérisson, J.-L.; Chauvin, Y. *Makromol. Chem.* **1971**, *141*, 161.

(7) Górski, M.; Szymańska-Buzar, T. *J. Mol. Catal. A* **2006**, *257*, 41.

(8) (a) Bencze, L.; Kraut-Vass, A.; Prókai, L. *J. Chem. Soc., Chem. Commun.* **1985**, 911. (b) Veige, A. S.; Wolczanski, P. T.; Lobkovsky, E. B. *Angew. Chem., Int. Ed.* **2001**, *40*, 3629.

(9) Handzlik, J.; Górski, M.; Szymańska-Buzar, T. *J. Mol. Struct. THEOCHEM* **2005**, *718*, 191.

(10) Handzlik, J.; Stosur, M.; Kochel, A.; Szymańska-Buzar, T. *Inorg. Chim. Acta* **2008**, *502*, 41.

(11) Tosh, E. K. M.Sc. Thesis, University of Regina, Regina, Canada, 2006.

(12) Arnesen, S. V.; Seip, H. M. *Acta Chem. Scand.* **1966**, *20*, 2711.

(13) Heinemann, F.; Schmidt, H.; Peters, K.; Thiery, D. *Z. Kristallogr.* **1992**, *198*, 123.

(14) Szymańska-Buzar, T.; Kern, K.; Downs, A. J.; Greene, T. M.; Morris, L. J.; Parsons, S. *New J. Chem.* **1999**, *23*, 407.

(15) Grevels, F.-W.; Jacke, J.; Betz, P.; Krüger, C.; Tsay, Y.-H. *Organometallics* **1989**, *8*, 293.

(16) Drew, M. G. B.; Baker, P. K.; Armstrong, E. M.; Fraser, S. G.; Muldoon, D. J.; Lavery, A. J.; Shawcross, A. *Polyhedron* **1995**, *14*, 617.

(17) *Gaussian 03, Revision C.02*; Frisch, M. J.; Trucks, G. W.; Schlegel, H. B.; Scuseria, G. E.; Robb, M. A.; Cheeseman, J. R.; Montgomery, J. A., Jr.; Vreven, T.; Kudin, K. N.; Burant, J. C.; Millam, J. M.; Iyengar, S. S.; Tomasi, J.; Barone, V.; Mennucci, B.; Cossi, M.; Scalmani, G.; Rega, N.; Petersson, G. A.; Nakatsuji, H.; Hada, M.; Ehara, M.; Toyota, K.; Fukuda, R.; Hasegawa, J.; Ishida, M.; Nakajima, T.; Honda, Y.; Kitao, O.; Nakai, H.; Klene, M.; Li, X.; Knox, J. E.; Hratchian, H. P.; Cross, J. B.; Bakken, V.; Adamo, C.; Jaramillo, J.; Gomperts, R.; Stratmann, R. E.; Yazyev, O.; Austin, A. J.; Cammi, R.; Pomelli, C.; Ochterski, J. W.; Ayala, P. Y.; Morokuma, K.; Voth, G. A.; Salvador, P.; Dannenberg, J. J.; Zakrzewski, V. G.; Dapprich, S.; Daniels, A. D.; Strain, M. C.; Farkas, O.; Malick, D. K.; Rabuck, A. D.; Raghavachari, K.; Foresman, J. B.; Ortiz, J. V.; Cui, Q.; Baboul, A. G.; Clifford, S.; Cioslowski, J.; Stefanov, B. B.; Liu, G.; Liashenko, A.; Piskorz, P.; Komaromi, I.; Martin, R. L.; Fox, D. J.; Keith, T.; Al-Laham, M. A.; Peng, C. Y.; Nanayakkara, A.; Challacombe, M.; Gill, P. M. W.; Johnson, B.; Chen, W.; Wong, M. W.; Gonzalez, C.; Pople, J. A. Gaussian, Inc.: Wallingford, CT, 2004.

(18) Becke, A. D. *J. Chem. Phys.* **1993**, *98*, 5648.

(19) Lee, C.; Yang, W.; Parr, R. G. *Phys. Rev. B* **1988**, *37*, 785.

(20) Becke, A. D. *Phys. Rev. A* **1988**, *38*, 3098.

(21) (a) Perdew, J. P. *Phys. Rev. B* **1986**, *33*, 8822. (b) Perdew, J. P. *Phys. Rev. B* **1986**, *34*, 7406.

(22) Møller, C.; Plesset, M. S. *Phys. Rev.* **1934**, *46*, 618.

(23) Bartlett, R. J. *J. Phys. Chem.* **1989**, *93*, 1697.

(24) Hay, P. J.; Wadt, W. R. *J. Chem. Phys.* **1985**, *82*, 299.

(25) (a) Bardo, R. D.; Ruedenberg, K. *J. Chem. Phys.* **1974**, *60*, 918. (b) Bardo, R. D.; Ruedenberg, K. *J. Chem. Phys.* **1974**, *60*, 932.

(26) Wadt, W. R.; Hay, P. J. *J. Chem. Phys.* **1985**, *82*, 284.

(27) Glukhotsev, M. N.; Pross, A.; McGrath, M. P.; Radom, L. *J. Chem. Phys.* **1995**, *103*, 1878.

(28) Hepperle, S. S.; Li, Q.; East, A. L. L. *J. Phys. Chem. A* **2005**, *109*, 10975.

(29) Baker, J. *J. Comput. Chem.* **1986**, *7*, 385.

(30) Szilagyi, R. K.; Frenking, G. *Organometallics* **1997**, *16*, 4807.

(31) (a) Suzuki, H.; Kakigano, T.; Fukui, H.; Tanaka, M.; Morooka, Y. *J. Organomet. Chem.* **1994**, *473*, 295. (b) Jia, G.; Ng, W. S.; Lau, C. P. *Organometallics* **1998**, *17*, 4538.

(32) (a) McClellan, W. R.; Hoehn, H. H.; Cripps, H. N.; Muetterties, E. L.; Howk, B. W. *J. Am. Chem. Soc.* **1961**, *83*, 1601. (b) Shigeyoshi, S.; Takeuchi, K.; Sugimoto, M. *Organometallics* **1997**, *16*, 2995.

CT800088E